Article

Interplay of Cellular mRNA, miRNA and Viral miRNA during Infection of a Cell

Vladimir P. Zhdanov

Boreskov Institute of Catalysis, Russian Academy of Sciences, Novosibirsk 630090, Russia; zhdanov@catalysis.ru
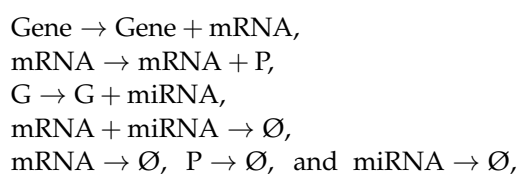
Abstract: The understanding of the kinetics of gene expression in cells infected by viruses is currently limited. As a rule, the corresponding models do not take viral microRNAs (miRNAs) into account. Such RNAs are, however, operative during the replication of some viruses, including, e.g., herpesvirus. To clarify the kinetics of this category (with emphasis on the information available for herpesvirus), I introduce a generic model describing the transient interplay of cellular mRNA, protein, miRNA and viral miRNA. In the absence of viral miRNA, the cellular miRNA is considered to suppress the populations of mRNA and protein due to association with mRNA and subsequent degradation. During infection, the viral miRNA suppresses the population of cellular miRNA and via this pathway makes the mRNA and protein populations larger. This effect becomes appreciable with the progress of intracellular viral replication. Using biologically reasonable parameters, I investigate the corresponding mean-field kinetics and show the scale of the effect of viral miRNAs on cellular miRNA and mRNA. The scale of fluctuations of the populations of these species is illustrated as well by employing Monte Carlo simulations.

Keywords: intracellular viral kinetics; gene expression; mRNA and miRNA; mean-field kinetic equations; Monte Carlo simulations

1. Introduction

Kinetic models are widely used in order to illustrate and clarify various aspects of gene expression in intact cells (reviewed in [1–6]; see also recent articles [7–11] and references therein) and during their infection by viruses (reviewed in [12–14]; see also [15–28] and references therein). The models of the former category are usually focused on proteins, mRNAs, and non-coding RNAs (ncRNAs), e.g., miRNAs. The models of the latter category typically operate with the populations of cellular proteins and mRNAs; and viral proteins, RNAs, or DNAs; and virions. Now, there is, however, evidence that various host miRNAs are involved in a cellular antiviral response and that active miRNAs can also be encoded by a viral genome and expressed in the host [29]. For COVID-19, for example, the corresponding literature is reviewed in [30,31]. Overall, the intracellular pathways, including host and viral miRNAs, are complex and not yet fully understood. The corresponding kinetic models with various feedbacks have in fact not been explored theoretically and obviously merit attention.

In this context, I can note that the interplay of viral miRNA and host mRNA and protein (P) was analyzed earlier theoretically [27] by using a four-variable kinetic mean-field model for the populations of these species, with the following mechanistic steps:

$$\text{Gene} \rightarrow \text{Gene} + \text{mRNA},$$
$$\text{mRNA} \rightarrow \text{mRNA} + \text{P},$$
$$\text{G} \rightarrow \text{G} + \text{miRNA},$$
$$\text{mRNA} + \text{miRNA} \rightarrow \varnothing,$$
$$\text{mRNA} \rightarrow \varnothing, \ \text{P} \rightarrow \varnothing, \ \text{and} \ \text{miRNA} \rightarrow \varnothing,$$

where Gene and G represent the host and viral genomes. The cellular ncRNA was, however, not taken there into account.
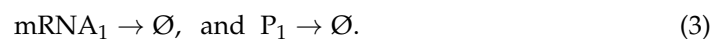
Herein, I present a more complete generic kinetic model describing the interplay of viral miRNAs and cellular mRNAs, miRNAs, and proteins. To validate this work, I can refer to the replication of herpesvirus, the formation of the corresponding viral miRNAs, and their interactions with cellular ncRNAs (see, e.g., experiments [32–34]); regarding antiviral miRNAs, see [35]). The cellular ncRNAs can influence the population of cellular mRNAs, and accordingly the population of the corresponding cellular proteins can be influenced as well.

As a general remark for introducing the math, I recall that in kinetic models of gene expression in cells, the formation and degradation of proteins, mRNAs, and ncRNAs are usually viewed as the key elementary steps [2–6]. In reality, these steps occur via numerous substeps [1]. In other words, the steps under consideration are almost always coarse-grained—i.e., a single step represents a few substeps—and each substep often represents in turn a few substeps of a lower level. The extent of detalization of steps and substeps depends on the goals of an analysis. Usually, a theoretical treatment has a few goals, and accordingly, the extent of detalization can be different even in one study. With this reservation, I first introduce below a set of steps in order to keep the links with numerous earlier theoretical models [2–6] and a relevant experiment [34] and then simplify them in order to keep the math compact and suitable for general readership (Section 2). The results of the corresponding mean-field calculations and Monte Carlo (MC) simulations are given afterwards (Section 3) and followed by the conclusion (Section 4).
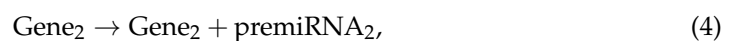
2. Methods

2.1. General Scheme

For genes of one type (as in the model under consideration), the steps resulting in the mRNA and protein formation are usually schematically presented as [2–6]

$$\text{Gene}_1 \rightarrow \text{Gene}_1 + \text{mRNA}_1, \tag{1}$$

$$\text{mRNA}_1 \rightarrow \text{mRNA}_1 + \text{P}_1, \tag{2}$$

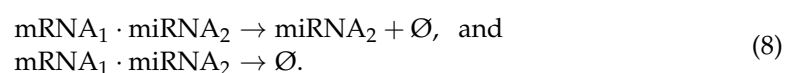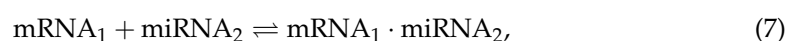$$\text{mRNA}_1 \rightarrow \varnothing, \ \text{ and } \ \text{P}_1 \rightarrow \varnothing. \tag{3}$$

Genes can be transcribed also into ncRNAs, or more specifically (in the context under consideration), into miRNAs, which are short compared to mRNA [6,36]. Mechanistically, it occurs via the formation of precursors (long premiRNAs); i.e., the corresponding steps can be represented as

$$\text{Gene}_2 \rightarrow \text{Gene}_2 + \text{premiRNA}_2, \tag{4}$$

$$\text{premiRNA}_2 \rightarrow \text{miRNA}_2, \tag{5}$$

$$\text{premiRNA}_2 \rightarrow \varnothing, \ \text{ and } \ \text{miRNA}_2 \rightarrow \varnothing. \tag{6}$$

Comparing steps (1) and steps (4) and (5), one can notice that the former step does not include pre-mRNA, whereas the latter steps contain pre-miRNA$_2$, and this might appear inconsistent because in reality the formation of mRNA includes pre-mRNA as well (see, e.g., Figure 1 in [1]). As in many other kinetic models of gene expression [2–6], I do not introduce the substeps including pre-mRNA because they are not coupled with other substeps and accordingly are not important in the context under consideration.

The conventional scheme of the interaction of mRNA and miRNA includes their reversible association and degradation [6,37],

$$\text{mRNA}_1 + \text{miRNA}_2 \rightleftharpoons \text{mRNA}_1 \cdot \text{miRNA}_2, \tag{7}$$

$$\begin{aligned} \text{mRNA}_1 \cdot \text{miRNA}_2 &\rightarrow \text{miRNA}_2 + \varnothing, \ \text{ and} \\ \text{mRNA}_1 \cdot \text{miRNA}_2 &\rightarrow \varnothing. \end{aligned} \tag{8}$$

As is usual in molecular biology, these steps resemble those of the classical enzyme kinetics (with $miRNA_2$ being the enzyme and $mRNA_1$ the substrate to be degraded).
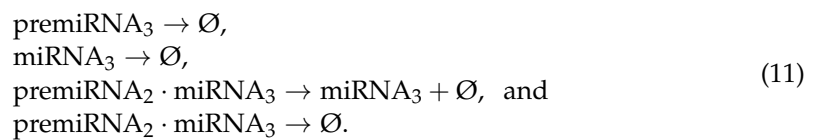
After infection of a cell, virions use the cellular machinery for the formation of various species needed for their replication. The corresponding steps are numerous. In the context under consideration, the attention can be focused on the viral genome transcription into viral pre-miRNA with subsequent conversion to viral miRNA (as, e.g., in the case of herpesvirus [34]),

$$G \to G + premiRNA_3 \quad \text{and} \quad premiRNA_3 \to miRNA_3, \tag{9}$$

association of viral miRNA with cellular pre-miRNA,

$$premiRNA_2 + miRNA_3 \rightleftharpoons premiRNA_2 \cdot miRNA_3, \tag{10}$$

and degradation of these species,

$$\begin{aligned} &premiRNA_3 \to \varnothing, \\ &miRNA_3 \to \varnothing, \\ &premiRNA_2 \cdot miRNA_3 \to miRNA_3 + \varnothing, \quad \text{and} \\ &premiRNA_2 \cdot miRNA_3 \to \varnothing. \end{aligned} \tag{11}$$

In addition, there are viral genome replication and degradation:

$$G \to 2G \quad \text{and} \quad G \to \varnothing. \tag{12}$$

The G replication is here represented as one coarse-grained lumped step. The G loss is shown as one lumped step as well. The latter step is assumed to describe all the channels of the loss, including the G degradation and the formation of premature and mature virions and their departure from a cell.

The mechanistic steps above do not contain the cellular DNA replication, and in the context of the analysis presented, this means that all the processes occur in a cell during one cell cycle. The focus on this situation is biologically reasonable and can be validated comparing the timescales of various processes occurring in human cells. In particular, the timescales of the formation and degradation of proteins, mRNA, and miRNA are typically shorter or comparable with one hour (see, e.g., Section 3.6 in [6] or [38]). The timescale of the viral genome replication is usually a few hours (see, e.g., Figure 2 for HIV-1 and IVA viruses in [21]). In contrast, the length of the cycle of human fast-dividing cells grown outside the body under optimal conditions is typically longer (approximately 24 h [38]), and the lengths of the cycles of many other cells which are relevant for infections are often much longer both in vivo and in vitro (see, e.g., the data for transformed human hepatocyte growth [39]). Taken together, this information means that the number of viral genomes formed in a cell during the cell cycle is often large, and accordingly, it makes sense to focus on this case.

2.2. Coarse-Grained Steps

The kinetic equations corresponding to the steps introduced above are somewhat cumbersome. To simplify the treatment, I keep steps (1)–(3) for the formation and degradation of $mRNA_1$ and P_1, steps for the $miRNA_2$ and $miRNA_3$ degradation (in (6) and (11)), and using one of the common approximations in the models of gene expression, replace steps (4), (5), and (9) for the $miRNA_2$ and $miRNA_3$ formation with two lumped steps,

$$Gene_2 \to Gene_2 + miRNA_2, \tag{13}$$

$$G \to G + miRNA_3. \tag{14}$$
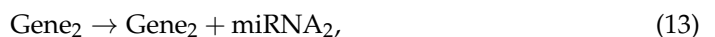
Along this line, I replace the mRNA$_1$-miRNA$_2$ association step (7) and the corresponding degradation steps (8) by one lumped step

$$\text{mRNA}_1 + \text{miRNA}_2 \rightarrow \varnothing. \tag{15}$$

By analogy, the premiRNA$_2$-miRNA$_3$ association step (10) and the corresponding degradation steps (11) are replaced by one lumped step as well:

$$\text{miRNA}_2 + \text{miRNA}_3 \rightarrow \varnothing. \tag{16}$$

In this framework, the intermediates, pre-miRNA$_2$ and pre-miRNA$_3$; and complexes, mRNA$_1 \cdot$ miRNA$_2$ and premiRNA$_2 \cdot$ miRNA$_3$, are not described explicitly, and accordingly, the degradation steps of these species ((8) and in (11)) can be excluded from the math. This procedure is intuitively clear. Mathematically, it is a matter of introduction of the effective rate constants (see, e.g., Section 4.2 in [6]).

2.3. Mean-Field Kinetic Equations

The coarse-grained scheme introduced above contains cellular mRNA$_1$, P$_1$, and miRNA$_2$; viral miRNA$_3$; and G. The corresponding populations are designated as n_1, n_p, n_2, n_3, and n_g. The conventional mean-field kinetic equations for the former four variables are as follows:

$$\begin{aligned}
dn_1/dt &= w_1 - k_1 n_1 - \kappa_{12} n_1 n_2, \\
dn_\text{p}/dt &= \kappa_\text{p} n_1 - k_\text{p} n_\text{p}, \\
dn_2/dt &= w_2 - k_2 n_2 - \kappa_{12} n_1 n_2 - \kappa_{23} n_2 n_3, \\
dn_3/dt &= \kappa_3 n_\text{g} - k_3 n_3 - \kappa_{23} n_2 n_3,
\end{aligned} \tag{17}$$

where w_1 and w_2 are the rates of formation of mRNA$_1$ and miRNA$_2$; κ_p is the rate constant of the P$_1$ formation; κ_3 is the rate constant of the miRNA$_3$ formation; κ_{12} and κ_{23} are the association rate constants; and k_1, k_p, k_2, and k_3 are the degradation rate constants.

According to (17), the P$_1$ population does not influence other populations, and under steady-state conditions this population is just proportional to the mRNA$_1$ population. Under such conditions, it can in principle be excluded from the analysis. I keep P$_1$ for possible extensions of the model. The key argument in favor of P$_1$ is that cellular and viral proteins are widely considered to be main regulators of virus fitness [22,41]. For example, one can assume that P$_1$ regulates the G growth and describe this effect formally by using, e.g., the Hill expression for κ_g (see below) or in more detail (provided the corresponding information is available).

In addition to (17), I need the equation describing the G replication. The initial phase of this process is expected to be close to exponential. Later on, the exponential growth of the G population is terminated (due to regulation of replication and/or exhaustion of cellular resources), and then this population may diminish (e.g., in the case of cell death). These features follow from numerous experiments with various virus-cell assays (for the types of assays, see [12]) and also from available kinetic models (see, e.g., [21,28] and references therein). In particular, one of the consequences of the exponential growth is that in the corresponding kinetics (e.g., those measured in assays), the logarithm of concentration is customarily shown as a function of time. Phenomenologically, the kinetics of this type can be described as

$$dn_\text{g}/dt = \kappa_\text{g}(1 - n_\text{g}/n_*)n_\text{g}, \tag{18}$$

where κ_g is the replication rate constant and n_* is the maximum G population. This equation predicts the exponential growth of the G population at $n_\text{g} \ll n_*$ with subsequent saturation $n_\text{g} \rightarrow n_*$. Formally, the two terms, $\kappa_\text{g} n_\text{g}$ and $\kappa_\text{g} n_\text{g}^2/n_*$, can be assumed to correspond to forward and backward reactions. Alternatively, the growth can be assumed to be limited by unspecified feedback, and $\kappa_\text{g}(1 - n_\text{g}/n_*)$ can considered to represent the effective n_g-

dependent replication rate constant. In the mean-field approximation, the equation is applicable in both cases.

Regarding the initial exponential growth predicted by (18), one can for analogy refer to frequently-observed exponential growth of bacteria (briefly reviewed in [42]). In the latter case, the deviations from the exponential growth are sometimes observed as well (briefly reviewed in [43]). Compared to bacterial or cellular DNA, the viral genomes are, however, relatively short, and by analogy with the formation of cellular mRNA and proteins (in the absence of regulation), one can expect that the initial first-order law in (18) is fairly accurate.

Concerning (18), I can add that cellular mRNAs, proteins, and miRNAs, and viral miRNAs, can influence the viral-genome growth due to feedback. In human herpesvirus 6A, for example, virus-encoded miR-aU14 selectively inhibits the processing of multiple miR-30 family members, subsequent activation of the miR-30-p53-DRP1 axis triggers a profound disruption of mitochondrial architecture, and this impairs induction of type I interferons and is necessary for both productive infection and virus reactivation [34]. Although the full-scale analysis of these steps is obviously very interesting, its realization is challenging. One of the already mentioned options is to introduce formal feedback of the Hill type [27,40]. For example, one can admit that the replication rate is positively or negatively regulated by P_1 and represent κ_g in Equation (18) for n_g, respectively, as

$$\kappa_g = \kappa_g^\circ + \kappa_g^* \frac{n_g^m}{K^m + n_p^m} \ \ \text{or} \ \ \kappa_g = \kappa_g^\circ + \kappa_g^* \frac{K^m}{K^m + n_p^m},$$

where κ_g°, κ_g^*, K, and m are the Hill parameters. To solve Equation (18), n_p should be expressed via n_g. It can be done by employing Equations (17) above or (19) below. This approach will, however, not really extend the understanding of the mechanistic details. For this reason, I focus on the interplay of $mRNA_1$, P_1, $miRNA_2$, and $miRNA_3$ and do not take the effect of these species on the G growth into account—i.e., Equation (18) describing the G replication is considered to be not coupled to Equations (17).

As already noticed, the G-replication timescale, $1/\kappa_g$ (Equation (18)), is longer than the timescales characterizing other steps (in (17)), and accordingly, the latter steps can be described in the steady-state approximation by setting $dn_1/dt = dn_p/dt = dn_2/dt = dn_3/dt = 0$. In this approximation, Equations (17) can be rewritten as

$$\begin{aligned}
n_1 &= w_1/(k_1 + \kappa_{12} n_2), \\
n_2 &= w_2/(k_2 + \kappa_{12} n_1 + \kappa_{23} n_3), \\
n_3 &= \kappa_3 n_g/(k_3 + \kappa_{23} n_2), \\
n_p &= \kappa_p n_1/k_p.
\end{aligned} \tag{19}$$

In these equations for n_1, n_p, n_2, and n_3, n_g can be considered to be a time-dependent governing parameter determined by (18) as

$$n_g = \frac{n_* \exp(\kappa_g t)}{n_* - 1 + \exp(\kappa_g t)}. \tag{20}$$

This expression shows explicitly n_g as a function of $\kappa_g t$. For any given n_g, the other populations, n_1, n_p, n_2, and n_3, are determined by (19). Thus, n_1, n_p, n_2, and n_3 can be calculated as a function of $\kappa_g t$ as well.

2.4. Stochasticity

Stochasticity arising in gene expression from fluctuations in transcription and translation has attracted interest for many years because of its implications for cellular regulation and non-genetic individuality (reviewed in [2,3]; see also recent articles [7,10] and references therein). Compared to conventional chemical systems, the role of fluctuations is here more appreciable because many mRNAs, ncRNAs, and proteins are present in low numbers per cell. During virus replication in cells, the numbers of viral genome, mRNA,

ncRNA, and protein copies are often low as well, especially in the beginning. Although the corresponding fluctuations have already been shown theoretically (see, e.g., [15,21,24,25]), the full-scale understanding of their role in real systems is still limited.

The mean-field equations presented above do not take fluctuations into account. To illustrate the scale of fluctuations, one can simulate the steps under consideration by using the MC technique. To simplify simulations, one can notice that the G population is typically smaller than the $mRNA_1$ and $miRNA_2$ populations and often smaller than the $miRNA_3$ population. This means that the generation of an additional G copy results in a rapid, appreciable increase or decrease in numbers of copies of other species at the mean-field level. Under such conditions, the fluctuations of the $mRNA_1$, P_1, $miRNA_2$, and $miRNA_3$ populations are related primarily to those of the G population, and accordingly, the MC technique, or more specifically, the standard Gillespie algorithm, can be used in order to describe only this population, i.e., n_g (Equation (18)), whereas the populations of other species can be tracked at any given n_g at the mean-field level by employing (19). The realization of the corresponding MC simulations depends slightly on the interpretation of Equation (18). To be specific, I consider that the G growth is limited by unspecified feedback so that $\kappa_g(1 - n_g/n_*)$ represents the effective replication rate constant. In this framework, the time interval corresponding the generation of an additional G copy is given by $\Delta t = \ln(q)/[\kappa_g(1 - n_g/n_*)n_g]$, where $0 < q \leq 1$ is a random number, and $\kappa_g(1 - n_g/n_*)n_g$ is the replication rate (in (18)).

3. Results and Discussion

3.1. Mean-Field Kinetics

The coarse-grained model introduced above is focused on five key species, including cellular $mRNA_1$, P_1, and $miRNA_2$; viral $miRNA_3$; and G. Equations (19) and (20) for the corresponding populations, n_1, n_p, n_2, n_3, and n_g, contain many kinetic parameters. In principle, the model can be used in order to describe real kinetics of infection of individual cells, and ideally, the parameters can/should be specified by using independent experiments. In practice, with the current state of the art, this is impossible because the available experimental data are far from sufficient. Under such circumstances, my goal is less ambitious. Specifically, I focus on the typical shape of the kinetics under consideration with biologically reasonable populations of various species. Following this line, I show below the populations of cellular $mRNA_1$ and $miRNA_2$, n_1 and n_2; viral $miRNA_3$, n_3; and G, n_g. The P_1 population, $n_p = \kappa_p n_1/k_p$ (in (19)), is not shown, because this population is just proportional to the $mRNA_1$ population.

To keep the presentation of the result transparent and compact, I set the rate constants of degradation of $mRNA_1$, $miRNA_2$, and $miRNA_3$ to be equal (to k), i.e., $k_1 = k_p = k_2 = k_3 \equiv k$. In addition, I took into account that, in fact, the solution of Equations (19) depends only on the ratios of various rate constants, and accordingly, one can operate by using these ratios. The corresponding dimensionless values should be chosen to have biologically reasonable populations of $mRNA_1$, $miRNA_2$, and $miRNA_3$. In human cells, the populations of these species are well known to be in a wide range, roughly from 10 to 10^4 per cell (see, e.g., [6]). To be in this range, I used somewhat arbitrarily the following set of the parameters: $w_1/k = 200$, $w_2/k = 400$, $\kappa_{12}/k = 0.01$, $\kappa_{23}/k = 0.01$, and $\kappa_3/k = 10$.

The steady-state dependence of the $mRNA_1$, $miRNA_2$, and $miRNA_3$ populations, n_1, n_2, and n_3, on the G population, n_g, predicted by (19), with the chosen values of the kinetic parameters is shown in Figure 1. The temporal mean-field kinetics under consideration; or more specifically, the $mRNA_1$, $miRNA_2$, $miRNA_3$, and G populations calculated according to Equations (19) and (20) as a function of $\kappa_g t$ are exhibited in Figure 2.

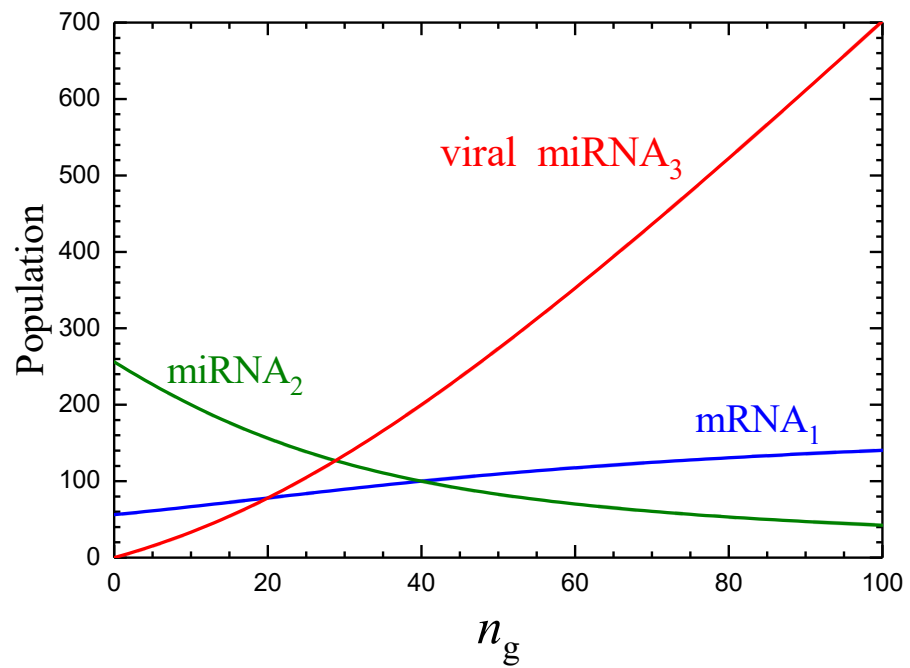**Figure 1.** $mRNA_1$, $miRNA_2$, and $miRNA_3$ populations as a function of the G population according to (19) with $w_1/k = 200$, $w_2/k = 400$, $\kappa_{12}/k = \kappa_{23}/k = 0.01$, and $\kappa_3/k = 10$. The model contains also the P_1 population. The latter population (not shown here and below in other figures) is just proportional to the $mRNA_1$ population.
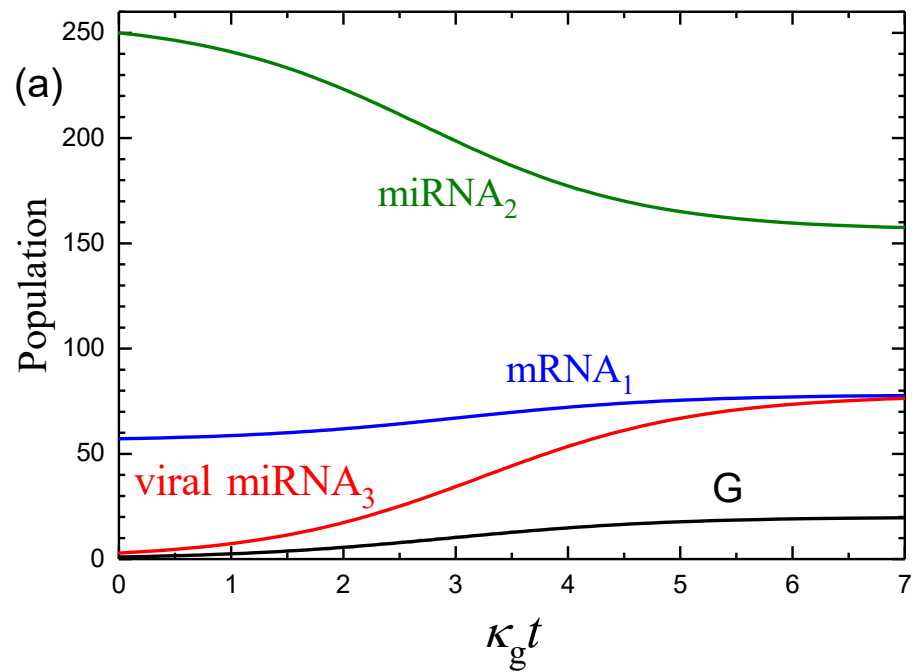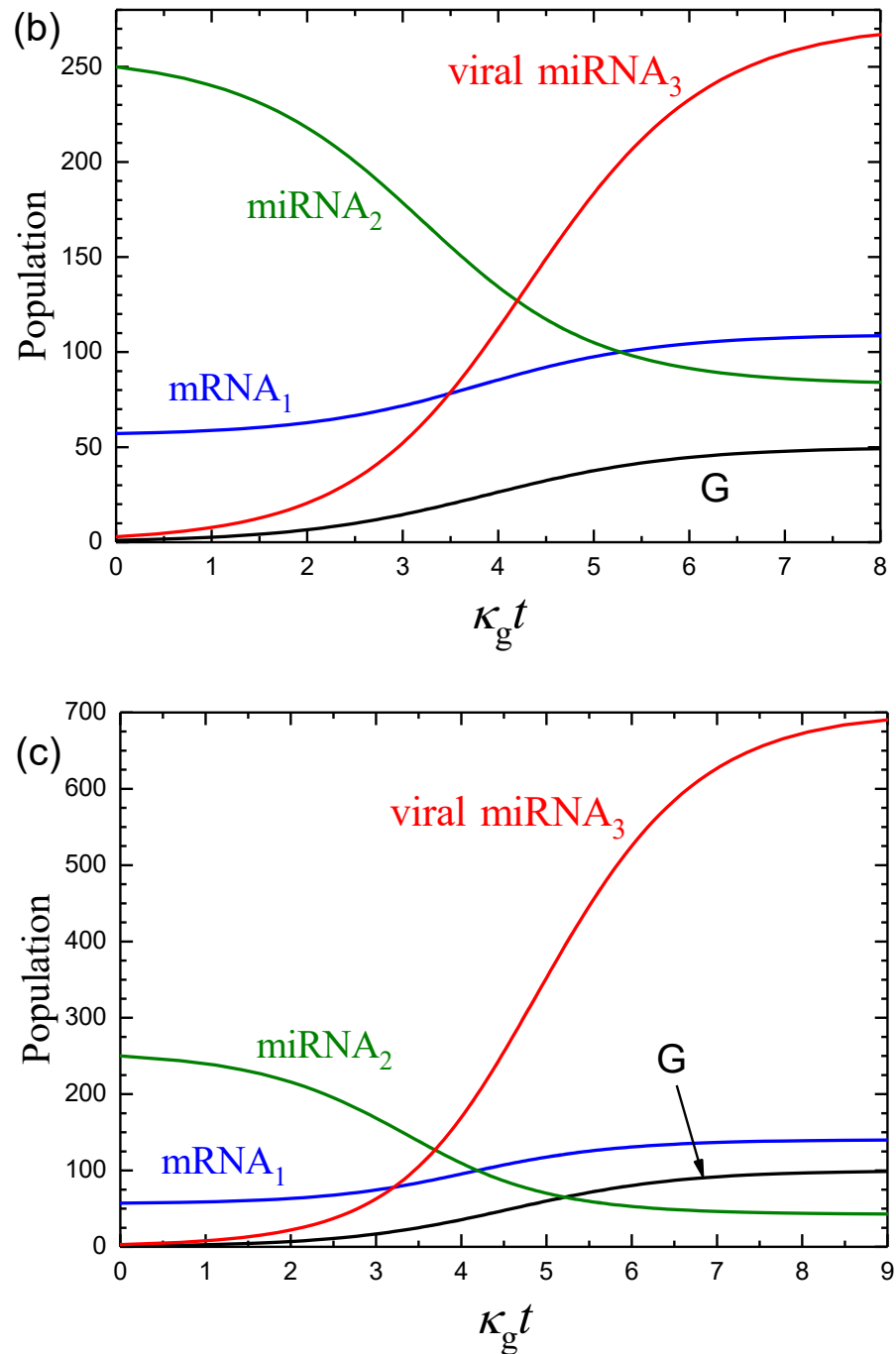

Figure 2. *Cont.*

Figure 2. $mRNA_1$, $miRNA_2$, $miRNA_3$, and G and populations as a function of $\kappa_g t$ according to Equations (19) and (20) with $n_g(0) = 1$ for $n_* = 20$ (**a**), 50 (**b**), and 100 (**c**) and the other parameters ($w_1/k = 200$, $w_2/k = 400$, $\kappa_{12}/k = \kappa_{23}/k = 0.01$, and $\kappa_3/k = 10$) as in Figure 1. In this model, the infection of a cell is possible by one virion [$n_g(0) = 1$], in agreement with the so-called independent action hypothesis [40]. In the absence of virus ($n_g = 0$ and $n_3 = 0$), the $mRNA_1$ and $miRNA_2$ population are $n_1 = 56$ and $n_2 = 256$ (Figure 1).

To interpret the kinetics shown in Figures 1 and 2, one can notice that in the absence of the $mRNA_1$-$miRNA_2$ and $miRNA_2$-$miRNA_3$ interactions, the model with the chosen parameters predicts that the $mRNA_1$ and $miRNA_2$ populations should be $n_1 = w_1/k = 200$ and $n_2 = w_2/k = 400$. These values are typical for abundant mRNAs and miRNAs. In the absence of the $miRNA_2$–$miRNA_3$ interaction, the $mRNA_1$–$miRNA_2$ interaction results

in a decrease in the $mRNA_1$ and $miRNA_2$ populations down to $n_1 = 56$ and $n_2 = 256$ (this case corresponds to $n_g = 0$ in Figure 1). The scale of this decrease is typical for the mRNA–miRNA interaction. In the presence the $miRNA_2$–$miRNA_3$ interaction, the effect of $miRNA_3$ on the $mRNA_1$ and $miRNA_2$ populations is first nearly negligible as long as the $miRNA_3$ population is low. With increasing G and $miRNA_3$ populations, the effect of $miRNA_3$ on the $miRNA_2$ population becomes larger, and the latter population drops, and accordingly, the suppression of the $mRNA_1$ population becomes weaker. Thus, the $mRNA_1$ population grows. If the $miRNA_3$ population eventually reaches an appreciable value (as, e.g., in Figure 2c), the $mRNA_1$ population increases up to 140, i.e., by a factor of 2.

To illustrate the effect of the variation of parameters on the kinetics, it is instructive to increase the rate constants of the formation of $mRNA_1$, $miRNA_2$, and $miRNA_3$ by one order of magnitude up to $w_1/k = 2000$, $w_2/k = 4000$, and $\kappa_3/k = 100$ and to keep other parameters the same as above ($\kappa_{12}/k = 0.01$ and $\kappa_{23}/k = 0.01$). In this case, the initial $miRNA_2$ population becomes larger, roughly by one order of magnitude (cf. Figures 2b and 3). The initial $mRNA_1$ population increases only by a factor of 2 because the increase in w_1/k is compensated by the increase in the initial $miRNA_2$ population. Globally, the kinetics are qualitatively the same. Quantitatively, the final relative increase in the $mRNA_1$ population and decrease in the $miRNA_2$ population (compared to the initial values) are more appreciable.

For arbitrary parameters, the relative roles of various processes can be clarified by analogy under the steady-state conditions (by using (19), first in the case before infection (with $n_g = 0$) and then for an appreciable n_g, e.g., 100, or under transient conditions (by employing (19) and (20)).
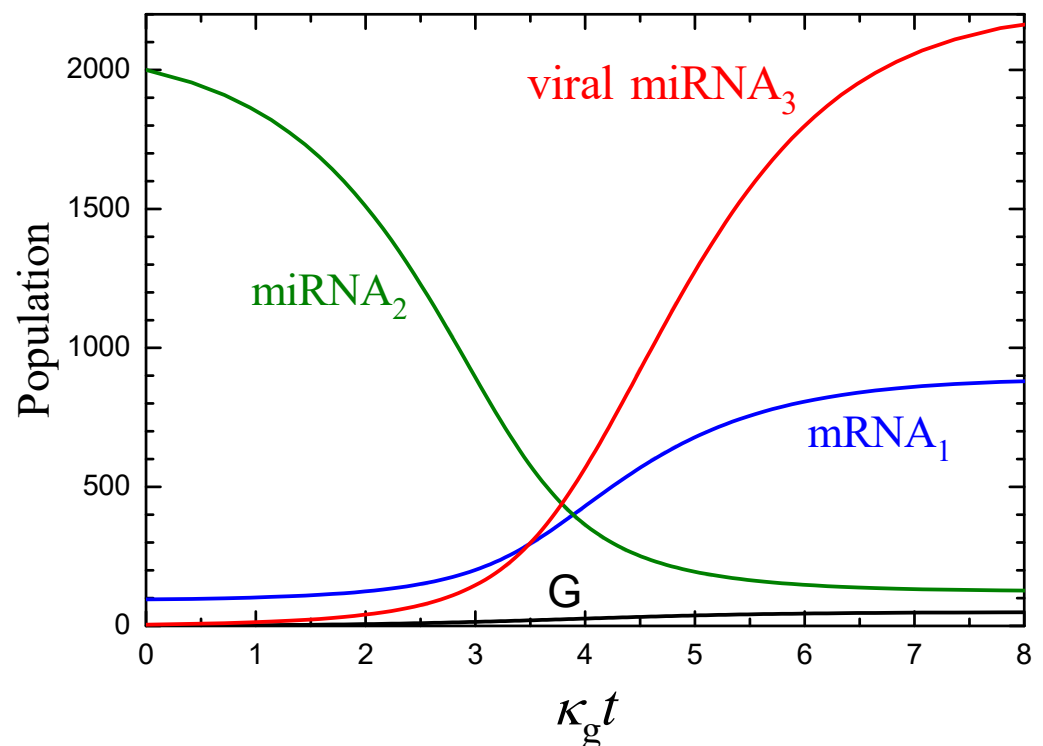

Figure 3. As Figure 2 for $w_1/k = 2000$, $w_2/k = 4000$, $\kappa_{12}/k = \kappa_{23}/k = 0.01$, $\kappa_3/k = 100$, and $n_* = 50$. Compared to the parameters used to construct Figure 2, w_1/k, w_2/k, and κ_3/k are here increased by one order of magnitude, whereas $n_* = 50$ is as in Figure 2b. In the absence of virus ($n_g = 0$ and $n_3 = 0$), the $mRNA_1$ and $miRNA_2$ population are $n_1 = 91$ and $n_2 = 2091$.

3.2. Monte Carlo Simulations

Typical temporal MC kinetics (Figure 4) exhibit appreciable fluctuations. Such kinetics can be characterized by calculating average populations, $\langle n \rangle$, and the corresponding standard deviations (Figure 5),

$$\sigma = \langle (\Delta n)^2 \rangle^{1/2}. \tag{21}$$

To interpret the results presented (Figure 5), I recall that in the context of gene expression in cells, each standard deviation (e.g., that corresponding to protein) is usually represented as a sum of three counterparts (see, e.g., [7] and note that the terminology I use is slightly different),

$$\sigma = \sigma_{\text{in}} + \sigma_{\text{ex}} + \sigma_{\text{div}}, \tag{22}$$

where σ_{in} is the intrinsic part (under steady-state conditions, this term is associated with Poisson noise); σ_{ex} is the extrinsic part related to regulation, or in other words, to the upstream noise (e.g., the fluctuations in mRNA copy number in the case of protein); and σ_{div} is the part related to partitioning noise due to the cell division. The Poisson distribution is well known to yield

$$\sigma_{\text{P}} = \langle n \rangle^{1/2}, \tag{23}$$

and under steady-state conditions with detailed balance, one is expected to have $\sigma = \sigma_{\text{in}} = \sigma_{\text{P}}$. Using $\langle n \rangle$, σ_{P} can formally be calculated under transient conditions as well (Equation (23)). In the latter case, σ can deviate from σ_{P}.
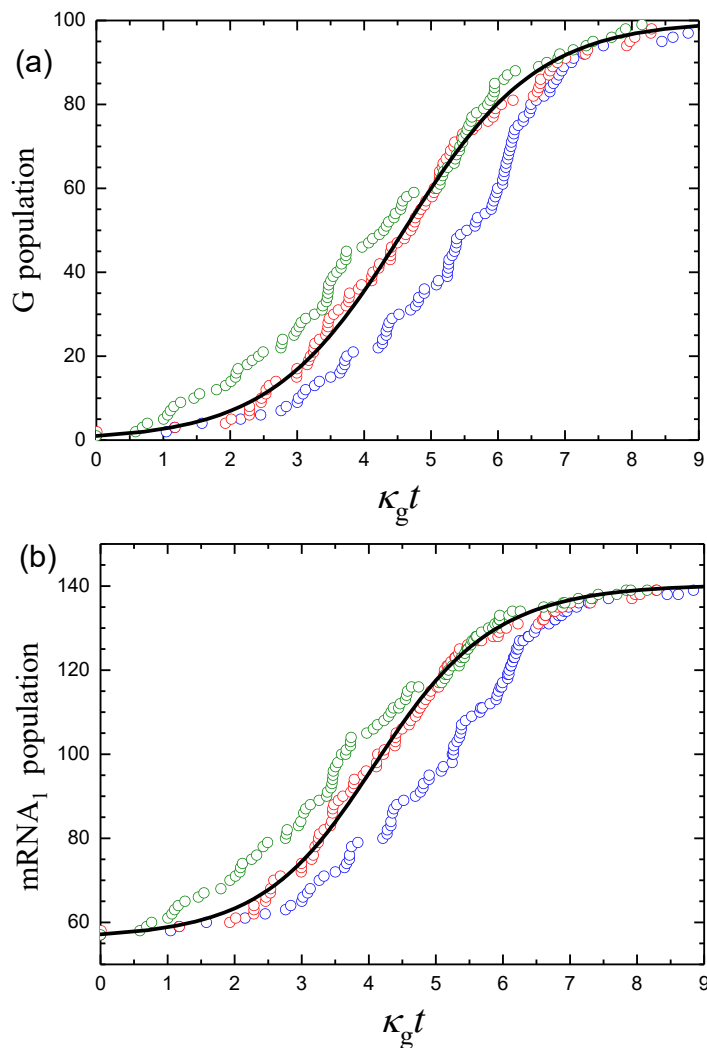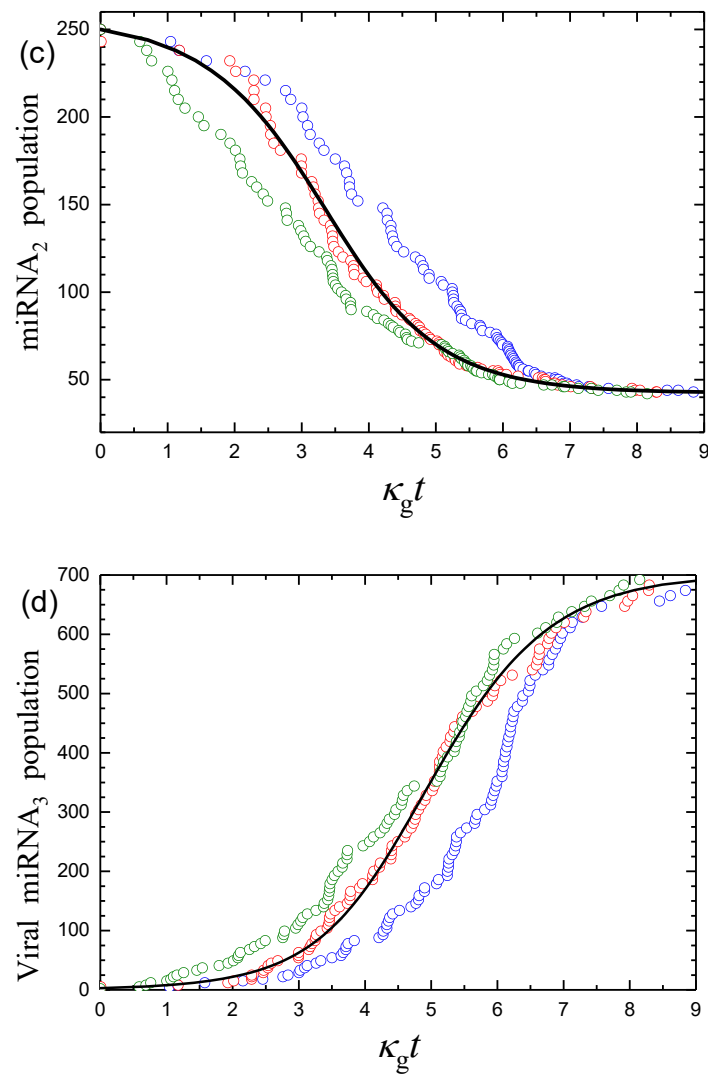

Figure 4. *Cont.*

Figure 4. (**a**) G, (**b**) mRNA$_1$, (**c**) miRNA$_2$, and (**d**) miRNA$_3$ populations as a function of $\kappa_{\mathrm{g}}t$ for $n_{\mathrm{g}}(0) = 1$. The mean-field kinetics calculated according to Equations (19) and (20) are shown by solid lines. Open circles exhibit three runs of the corresponding MC kinetics. The parameters are as in the case of Figure 2c.
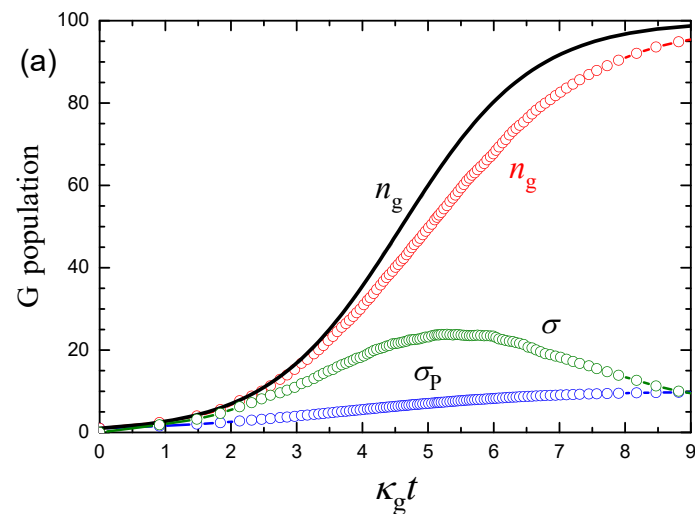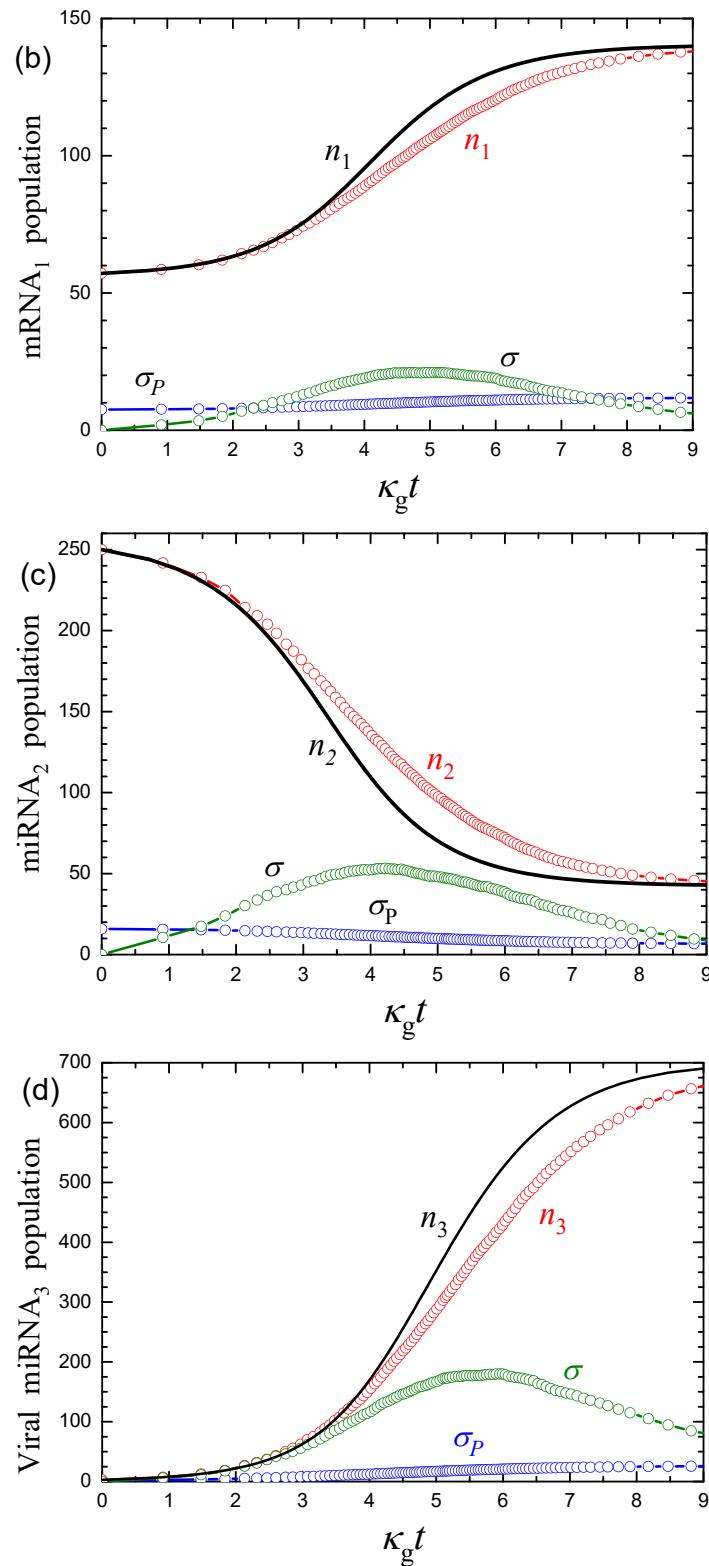

Figure 5. *Cont.*

Figure 5. (**a**) G, (**b**) mRNA$_1$, (**c**) miRNA$_2$, and (**d**) miRNA$_3$ kinetics as a function of $\kappa_g t$ for $n_g(0) = 1$. The mean-field populations (Equations (19) and (20)) are shown by solid lines. The averaged MC populations, standard deviations (Equation (21)), and Poissonian deviations (Equation (23)) shown by open circles were calculated by using 100 MC runs (as those exhibited in Figure 4).

In the model under consideration, the growth and division of cells are ignored, and accordingly, $\sigma_{\text{div}} = 0$ for all the species. The viral genome replication (step (12)) is consid-

ered to be independent of $mRNA_1$, P, $miRNA_2$, and $miRNA_3$—i.e., there is no regulation ($\sigma_{ex} = 0$)—and accordingly, the fluctuations are intrinsic, i.e., $\sigma = \sigma_{in}$. In contrast, $mRNA_1$, P, $miRNA_2$, and $miRNA_3$ are described at the mean-field level at each G copy number; i.e., the fluctuations of these species are related to those of the G population, and this means that $\sigma_{in} = 0$ and $\sigma = \sigma_{ex}$.

The simulations show that for G replication, σ is close to σ_P in the beginning and end of the kinetics, and larger than σ_P by a factor of three in the medium, where the G growth is fastest (Figure 5a). The $miRNA_3$ population is directly dependent on the G population, and here σ is much larger than σ_P (Figure 5d). The $mRNA_1$ and $miRNA_2$ population are indirectly dependent on the G population, and for them σ is smaller than σ_P in the beginning, smaller than or comparable to σ_P in the end, and appreciably larger than σ_P in the medium of the kinetics (Figure 5b,c). Thus, the scales of the maximal fluctuations of the $mRNA_1$, $miRNA_2$, and $miRNA_3$ populations are rather appreciable compared to σ_P. As already noticed, the reason for this feature is that the fluctuations of the populations of these species are related directly or indirectly to those of the G population. The latter population is relatively small, the fluctuations of this population with respect to its average value (the corresponding measure is $\sigma / \langle n \rangle$) are relatively large, and accordingly, the fluctuations of other populations are large as well.

4. Conclusions

Viral miRNAs can influence the kinetics of gene expression during infection of cells. This is an interesting example of transient kinetics of gene expression. In this study, I have presented a generic kinetic model and results of mean-field calculations and MC simulations illustrating the specifics of the interplay of viral miRNAs and cellular mRNAs, proteins, and miRNAs. The predicted type and scale of the effect of viral miRNA on cellular species are in qualitative agreement with the experiments reported for herpesvirus [34]. Quantitative theoretical analysis of the experiments is now hardly possible, because, as it often happens, the reported experimental data viewed from the perspective of the theory are incomplete.

Finally, I can note that the model presented can be extended in various directions. (i) For example, the model implies that the protein formed after translation of cellular mRNA does not regulate the formation of mRNA and other species. In reality, this regulation can take place, and it can result in more complex kinetics, including, e.g., bistability or oscillations [6]. (ii) The regulation of the replication of viral genomes can be taken into account (in more detail compared to [27,40]). (iii) Another extension can be aimed at more detailed analysis of what may happen at high intracellular population of viral genomes in the limit when the genome kinetic is not exponential (in the spirit of Ref. [21]). (iv) The cell cycle (or death) can be introduced into the treatment as well (in the spirit of references [44–46]). (v) Stochastic effects can be analyzed in more detail. (vi) All these extensions ((i)–(v)) can be done at the level of a few species. The specifics of miRNAs is that each such species can associate with various mRNAs [47], and the corresponding genetic networks can include multiple steps (up to one hundred). Such large networks can be analyzed as well.

Institutional Review Board Statement: Not applicable.

Informed Consent Statement: Not applicable.

Data Availability Statement: The data presented in this study are available in the article.

Conflicts of Interest: The author declares no conflict of interest.

References

1. Orphanides, G.; Reinber, D. A unified theory of gene expression. *Cell* **2002**, *108*, 439–451. [CrossRef] [PubMed]
2. Kaern, M.; Elston, T.C.; Blake, W.J.; Collins, J.J. Stochasticity in gene expression: From theories to phenotypes. *Nat. Rev. Genet.* **2005**, *6*, 451–464. [CrossRef]
3. Paulsson, J. Models of stochastic gene expression. *Phys. Life Sci.* **2005**, *2*, 157–175. [CrossRef]
4. Karlebach, G.; Shamir, R. Modelling and analysis of gene regulatory networks. *Nat. Rev. Molec. Cell Biol.* **2008**, *9*, 771–780. [CrossRef] [PubMed]
5. Vilar, J.M.G.; Saiz, L. Systems biophysics of gene expression. *Biophys. J.* **2013**, *104*, 2574–2585. [CrossRef]
6. Zhdanov, V.P. Kinetic models of gene expression including non-coding RNAs. *Phys. Rep.* **2011**, *500*, 1–42. [CrossRef]
7. Lin, J.; Amir, A. Disentangling intrinsic and extrinsic gene expression noise in growing cells. *Phys. Rev. Lett.* **2021**, *126*, 078101. [CrossRef]
8. Matsushita, Y.; Hatakeyama, T.S.; Kaneko, K. Dynamical systems theory of cellular reprogramming. *Phys. Rev. Res.* **2022**, *4*, L022008. [CrossRef]
9. Silverthorne, T.; Oh, E.S.; Stinchcombe, A.R. Promoter methylation in a mixed feedback loop circadian clock model. *Phys. Rev. E* **2022**, *105*, 034411. [CrossRef]
10. Chen, M.; Luo, S.; Cao, M.; Guo, C.; Zhou, T.; Zhang, J. Exact distributions for stochastic gene expression models with arbitrary promoter architecture and translational bursting. *Phys. Rev. E* **2022**, *105*, 014405. [CrossRef]
11. Szavits-Nossan, J.; Grima, R. Mean-field theory accurately captures the variation of copy number distributions across the mRNA life cycle. *Phys. Rev. E* **2022**, *105*, 014410. [CrossRef] [PubMed]
12. Handel, A.; Liao, L.E.; Beauchemin, C.A.A. Progress and trends in mathematical modelling of influenza A virus infections. *Curr. Opin. Syst. Biol.* **2018**, *12*, 30–36. [CrossRef]
13. Yin, J.; Redovich, J. Kinetic modeling of virus growth in cells. *Microbiol. Mol. Biol. Rev.* **2018**, *82*, e00066-17. [CrossRef] [PubMed]
14. Goyal, A.; Liao, E.; Perelson, A.S. Within-host mathematical models of hepatitis B virus infection: past, present, and future. *Curr. Opin. Syst. Biol.* **2019**, *18*, 27–35. [CrossRef]
15. Srivastava, R.; You, L.; Summers, J.; Yin, J. Stochastic vs. deterministic modeling of intracellular viral kinetics. *J. Theor. Biol.* **2002**, *218*, 309–324. [CrossRef]
16. Sidorenko, Y.; Reichl, U. Structured model of influenza virus replication in MDCK cells. *Biotechn. Bioing.* **2004**, *88*, 1–14. [CrossRef]
17. Sidorenko, Y.; Voigt, A.; Schulze-Horsel, J.; Reichl, U.; Kienle, A. Stochastic population balance modeling of influenza virus replication in vaccine production processes. II. Detailed description of the replication mechanism. *Chem. Eng. Sci.* **2008**, *63*, 2299–2304. [CrossRef]
18. Sardanyes, J.; Sole, R.V.; Elena, S.F. Replication mode and landscape topology differentially affect RNA virus mutational load and robustness. *J. Virol.* **2009**, *83*, 12579–12589. [CrossRef]
19. Rodrigo, G.; Carrera, J.; Jaramillo, A.; Elena, S.F. Optimal viral strategies for bypassing RNA silencing. *J. Roy. Soc. Interface* **2011**, *8*, 257–268. [CrossRef]
20. Sardanyes, J.; Martinez, F.; Daros, J.-A.; Elena, S.F. Dynamics of alternative modes of RNA replication for positive-sense RNA viruses. *J. Roy. Soc. Interface* **2012**, *9*, 768–776. [CrossRef]
21. Andreu-Moreno, I.; Bou, J.-V.; Sanjuan, R. Cooperative nature of viral replication. *Sci. Adv.* **2020**, *6*, eabd4942. [CrossRef] [PubMed]
22. Lopacinski, A.B.; Sweatt, A.J.; Smolko, C.M.; Gray-Gaillard, E.; Borgman, C.A.; Shah, M.; Janes, K.A. Modeling the complete kinetics of coxsackievirus B3 reveals human determinants of host-cell feedback. *Cell Syst.* **2021**, *12*, 304–323.e13. [CrossRef] [PubMed]
23. Chhajer, H.; Rizvi, V.A.; Roy, R. Life cycle process dependencies of positive-sense RNA viruses suggest strategies for inhibiting productive cellular infection. *J. Roy. Soc. Interface* **2021**, *18*, 20210401. [CrossRef] [PubMed]
24. Zhdanov, V.P. Stochastic kinetics of reproduction of virions inside a cell. *BioSystems* **2004**, *77*, 143–150. [CrossRef] [PubMed]
25. Zhdanov, V.P. Monte Carlo simulation of bifurcation in the intracellular viral kinetics. *Phys. Biol.* **2005**, *2*, 46–50. [CrossRef]
26. Zhdanov, V.P. Intracellular viral kinetics limited by the supply of amino acids for synthesis of viral proteins. *BioSystems* **2009**, *97*, 117–120. [CrossRef]
27. Zhdanov, V.P. Interplay of viral miRNAs and host mRNAs and proteins. *Cent. Eur. J. Phys.* **2011**, *9*, 1366–1371. [CrossRef]
28. Zhdanov, V.P. Initial phase of replication of plus-stranded RNA viruses. *Biophys. Rev. Lett.* **2018**, *13*, 93–108. [CrossRef]
29. Bruscella, P.; Bottini, S.; Baudesson, C.; Pawlotsky, J.M.; Feray, C.; Trabucchi, M. Viruses and miRNAs: More friends than foes. *Front. Microbiol.* **2017**, *8*, 824. [CrossRef]
30. Geraylow, K.R.; Hemmati, R.; Kadkhoda, S.; Ghafouri-Fard, S. miRNA expression in COVID-19. *Gene Rep.* **2022**, *28*, 101641. [CrossRef]
31. Khan, M.A.-A.-K.; Sany, M.R.U.; Islam, M.S.; Islam, A.B.M.M.K. Epigenetic regulator miRNA pattern differences among SARS-CoV, SARS-CoV-2, and SARS-CoV-2 world-wide isolates delineated the mystery behind the epic pathogenicity and distinct clinical characteristics of pandemic COVID-19. *Front. Genet.* **2020**, *11*, 765. [CrossRef] [PubMed]
32. Pfeffer, S.; Zavolan, M.; Grasser, F.A.; Chien, M.; Russo, J.J.; Ju, J.; John, B.; Enright, A.J.; Marks, D.; Sander, C.; et al. Identification of virus-encoded microRNAs. *Science* **2004**, *304*, 734–736. [CrossRef] [PubMed]

33. Cai, X.; Lu, S.; Zhang, Z.; Gonzalez, C.M.; Damania, B.; Cullen, B.R. Kaposi's sarcoma-associated herpesvirus expresses an array of viral microRNAs in latently infected cells. *Proc. Natl. Acad. Sci. USA* **2005**, *102*, 5570–5575. [CrossRef]

34. Hennig, T.; Prusty, A.B.; Kaufer, B.B.; Whisnant, A.W.; Lodha, M.; Enders, A.; Thomas, J.; Kasimir, F.; Grothey, A.; Klein, T.; et al. Selective inhibition of miRNA processing by a herpesvirus-encoded miRNA. *Nature* **2022**, *605*, 539. [CrossRef] [PubMed]

35. Li, Q.; Lowey, B.; Sodroski, C.; Krishnamurthy, S.; Alao, H.; Cha, H.; Chiu, S.; El-Diwany, R.; Ghany, M.G.; Liang, T.J. Cellular microRNA networks regulate host dependency of hepatitis C virus infection. *Nat. Comm.* **2017**, *8*, 1789. [CrossRef] [PubMed]

36. Bartel, D.P. Metazoan microRNAs. *Cell* **2018**, *173*, 20–51. [CrossRef]

37. Levine, E.; Jacob, E.B.; Levine, H. Target-specific and global effectors in gene regulation by microRNA. *Biophys. J.* **2007**, *93*, L52–L54. [CrossRef]

38. Shamir, M.; Bar-On, Y.; Phillips, R.; Milo, R. SnapShot: Timescales in cell biology. *Cell* **2016**, *164*, 1302. [CrossRef]

39. Patra, T.; Bose, S.K.; Kwon, Y.-C.; Meyer, K.; Ray, R. Inhibition of p70 isoforms of S6K1 induces anoikis to prevent transformed human hepatocyte growth. *Life Sci.* **2021**, *265*, 118764. [CrossRef]

40. Zhdanov, V.P. Virology from the perspective of theoretical colloid and interface science. *Curr. Opin. Coll. Interf. Sci.* **2021**, *53*, 101450. [CrossRef]

41. Pasin, F.; Shan, H.; García, B.; Müller, M.; San León, D.; Ludman, M.; Fresno, D.H.; Fátyol, K.; Munné-Bosch, S.; Rodrigo, G.; et al. Abscisic acid connects phytohormone signaling with RNA metabolic pathways and promotes an antiviral response that is evaded by a self-controlled RNA virus. *Plant Comm.* **2020**, *1*, 100099. [CrossRef] [PubMed]

42. Iyer-Biswas, S.; Crooks, G.E.; Scherer, N.F.; Dinner, A.R. Universality in stochastic exponential growth. *Phys. Rev. Lett.* **2014**, *113*, 028101. [CrossRef] [PubMed]

43. Pandey, P.P.; Singh, H.; Jain, S. Exponential trajectories, cell size fluctuations, and the adder property in bacteria follow from simple chemical dynamics and division control. *Phys. Rev. E* **2020**, *101*, 062406. [CrossRef] [PubMed]

44. Beentjes, C.H.L.; Perez-Carrasco, R.; Grima, R. Exact solution of stochastic gene expression models with bursting, cell cycle and replication dynamics. *Phys. Rev. E* **2020**, *101*, 032403. [CrossRef]

45. Cao, Z.; Grima, R. Analytical distributions for detailed models of stochastic gene expression in eukaryotic cells. *Proc. Natl. Acad. Sci. USA* **2020**, *117*, 4682–4692. [CrossRef]

46. Dessalles, R.; Fromion, V.; Robert, P. Models of protein production along the cell cycle: An investigation of possible sources of noise. *PLoS ONE* **2020**, *15*, e0226016. [CrossRef]

47. Zhdanov, V.P. Conditions of appreciable influence of microRNA on a large number of target mRNAs. *Molec. BioSyst.* **2009**, *5*, 638–643. [CrossRef]